ARTICLE
Journal of Cellular Biochemistry 113:3773–3787 (2012)

Journal of Cellular Biochemistry

Caveolin-1 Regulates Proliferation and Osteogenic Differentiation of Human Mesenchymal Stem Cells

Natasha Baker,[1,2] Guofeng Zhang,[3] Yang You,[1] and Rocky S. Tuan[1,2*]

[1] *Cartilage Biology and Orthopaedics Branch, National Institute of Arthritis and Musculoskeletal and Skin Diseases, Bethesda, Maryland 20892*

[2] *Department of Orthopaedic Surgery, Center for Cellular and Molecular Engineering, School of Medicine, University of Pittsburgh, Pittsburgh, Pennsylvania 15219*

[3] *Biomedical Engineering and Physical Science Shared Resource, National Institute of Biomedical Imaging and Bioengineering, National Institutes of Health, Department of Health and Human Services, Bethesda, Maryland 20892*

ABSTRACT

Caveolin-1 is a scaffolding protein of cholesterol-rich caveolae lipid rafts in the plasma membrane. In addition to regulating cholesterol transport, caveolin-1 has the ability to bind a diverse array of cell signaling molecules and regulate cell signal transduction in caveolae. Currently, there is little known about the role of caveolin-1 in stem cells. It has been reported that the caveolin-1 null mouse has an expanded population of cells expressing stem cell markers in the gut, mammary gland, and brain, suggestive of a role for caveolin-1 in stem cell regulation. The caveolin-1 null mouse also has increased bone mass and an increased bone formation rate, and its bone marrow-derived mesenchymal stem cells (MSCs) have enhanced osteogenic potential. However, the role of caveolin-1 in human MSC osteogenic differentiation remains unexplored. In this study, we have characterized the expression of caveolin-1 in human bone marrow derived MSCs. We show that caveolin-1 protein is enriched in density gradient-fractionated MSC plasma membrane, consisting of ~100 nm diameter membrane-bound vesicles, and is distributed in a punctate pattern by immunofluoresence localization. Expression of caveolin-1 increases in MSCs induced to undergo osteogenic differentiation, and siRNA-mediated knockdown of caveolin-1 expression enhances MSC proliferation and osteogenic differentiation. Taken together, these findings suggest that caveolin-1 normally acts to regulate the differentiation and renewal of MSCs, and increased caveolin-1 expression during MSC osteogenesis likely acts as a negative feedback to stabilize the cell phenotype. J. Cell. Biochem. 113: 3773–3787, 2012. © 2012 Wiley Periodicals, Inc.

KEY WORDS: CAVEOLIN-1, CAVEOLAE; MESENCHYMAL STEM CELLS; OSTEOGENESIS; PLASMA MEMBRANE; CELL SIGNALING

The organization of cell surface receptors and signaling molecules is an important determinant of cell signal transduction. Lipid rafts are microdomains in the plasma membrane that regulate cell surface protein trafficking. Caveolae are a subtype of lipid raft visible by electron microscopy as flask shaped invaginations in the cell surface membrane [Palade, 1953; Yamada, 1955]. Caveolae are enriched in cholesterol and are distinguished from other types of lipid raft by the presence of caveolin scaffolding proteins that are essential for caveolae formation and cholesterol binding [Rothberg et al., 1992; Fra et al., 1995; Murata et al., 1995]. There are three caveolin proteins. Caveolin-1 is most highly expressed in mouse adipose tissue and lung tissue [Scherer et al., 1994, 1996], while caveolin-3 is expressed in heart and skeletal muscle [Song et al., 1996b; Tang et al., 1996]. Caveolin-2 is usually co-expressed with caveolin-1 and appears unable to form caveolae in the absence of caveolin-1 [Scherer et al., 1996; Razani et al., 2001]. The caveolin proteins form a hairpin loop in the cell membrane with their N- and C-termini remaining in the cell

The authors have no conflicts of interest to declare.

Additional supporting information may be found in the online version of this article.

Grant sponsor: Intramural Research Program of the National Institutes of Health; Grant number: Z01 AR 41131; Grant sponsor: Pennsylvania Department of Health PADoH; Grant number: SAP 4100050913.

*Correspondence to: Dr. Rocky S Tuan, Department of Orthopaedic Surgery, Center for Cellular and Molecular Engineering, School of Medicine, University of Pittsburgh, 450 Technology Drive, Room 221, Pittsburgh, PA 15219-3143. E-mail: rst13@pitt.edu

Manuscript Received: 29 June 2012; Manuscript Accepted: 5 July 2012

Accepted manuscript online in Wiley Online Library (wileyonlinelibrary.com): 13 July 2012

DOI 10.1002/jcb.24252 • © 2012 Wiley Periodicals, Inc.

cytoplasm [Dupree et al., 1993; Monier et al., 1995]. The cytoplasmic portion of the caveolin-1 protein contains a caveolin scaffolding domain (CSD) sequence that can bind many different cell signaling molecules as reviewed elsewhere [see reviews by Krajewska and Maslowska, 2004; Patel et al., 2008].

The various growth factor receptors and signaling molecules that localize to caveolae and/or interact with caveolin-1 include the platelet-derived growth factor receptor (PDGFR) and the epidermal growth factor receptor (EGFR), G-protein coupled receptors, G-protein α and β subunits, Src, endothelial nitric oxide synthase (eNOS), and proteins in the Ras-p42/44 map kinase and PI3K-Akt pathways [Krajewska and Maslowska, 2004; Patel et al., 2008]. In some cases this association may enhance signaling, probably by bringing signaling components in close proximity of one another as proposed by the caveolin-signaling hypothesis [Lisanti et al., 1994]. However, association of proliferative signaling molecules with caveolin-1 is usually inhibitory. Consequently, caveolin-1 expression is inversely associated with cellular transformation and proliferative signaling in NIH3T3 cells [Engelman et al., 1997; Galbiati et al., 1998] and is associated with growth arrest and cell senescence [Galbiati et al., 2001; Volonte et al., 2002].

As well as regulating cell proliferation and cell senescence, caveolin-1 regulates major developmental and differentiation signaling pathways, including Wnt/β-catenin signaling and bone morphogenic protein (BMP) signaling. Most of the studies investigating the influence of caveolin-1 on β-catenin signaling have taken over-expression and/or knockdown approaches in cells transfected with a TCF/LEF responsive luciferase reporter (TOP-FLASH) as a readout of β-catenin signaling. These studies have shown that caveolin-1 inhibits β-catenin signaling in various cell lines [Galbiati et al., 2000; Lu et al., 2003; Torres et al., 2007; Rodriguez et al., 2009; Mo et al., 2010] and some have shown caveolin-1 inhibits β-catenin signaling by sequestering it at the cell membrane [Galbiati et al., 2000; Torres et al., 2007; Rodriguez et al., 2009; Mo et al., 2010]. Elevated levels of active β-catenin protein in mammary gland and intestinal crypt cells in the caveolin-1 knockout mouse suggest that caveolin-1 may also inhibit Wnt/β-catenin signaling in vivo [Li et al., 2005; Sotgia et al., 2005]. Also, in zebrafish embryos over-expression of caveolin-1 mRNA inhibits β-catenin signaling [Mo et al., 2010]. Meanwhile, caveolin-1 interaction with the type II BMP receptor also regulates BMP signaling [Nohe et al., 2005; Wertz and Bauer, 2008].

Mesenchymal stem cells (MSCs) are multipotent stromal cells that have the capacity to differentiate into chondrocytes, osteoblasts, and adipocytes as well as have immunosuppressive effects on lymphocytes [see reviews by Kolf et al., 2007; Petrie Aronin and Tuan, 2010]. By virtue of their ease of isolation, plasticity, and immunomodulatory activity, MSCs have been considered a prime candidate cell type for tissue repair and regeneration. However, effective utilization of MSCs for tissue repair depends on proper control of their homing, differentiation, and proliferation. A large number of studies have focused on using external stimuli to direct MSC differentiation and behavior, including composition and structure of the culture substratum, mechanical activation, and treatment with soluble growth factors. However, little attention has been paid to the composition of the MSC membrane, which critically controls the cell's ability to respond to all of these environmental stimuli. Interestingly, the expression of genes related to caveolae-mediated endocytosis is upregulated in human bone marrow derived MSCs compared to hematopoietic stem cells (HSCs) and human embryonic stem (ES) cells [Ren et al., 2011], suggesting a functional role for this pathway in MSCs.

There is already some evidence that caveolin-1 may regulate stem cell activities. Increased populations of cells expressing stem cell markers in the gut, mammary gland, and brain of the caveolin-1 knockout mouse suggest that caveolin-1 may negatively regulate stem cell proliferation and/or regulate stem cell differentiation in vivo [Li et al., 2005; Sotgia et al., 2005; Jasmin et al., 2009]. It has also been noted that caveolin-1 knockout mice have a greater bone volume than their wild type counterparts, and that the bone marrow derived MSCs from these animals have enhanced osteogenic potential [Rubin et al., 2007]. This suggests that caveolin-1 may negatively regulate MSC osteogenesis. If the same is true in humans, levels of caveolin-1 expression in MSCs could have implications for the clinical application of MSCs for skeletal repair and regeneration.

In this study, we describe the expression of caveolin-1 mRNA and the localization of caveolin-1 protein in human bone marrow derived MSCs and the consequences of caveolin-1 knockdown on their proliferation and osteogenic differentiation. The results show that caveolin-1 is expressed in undifferentiated MSCs and that its expression becomes elevated during osteogenesis. Knockdown of caveolin-1 expression enhances MSC proliferation in standard growth medium and enhances osteogenesis induced by osteogenic medium. We postulate that caveolin-1 functions to suppress the growth and differentiation of undifferentiated MSCs, and upon cell differentiation caveolin-1 expression is upregulated to stabilize the cell phenotype and reduce cell plasticity and renewal potential.

MATERIALS AND METHODS

TISSUE COLLECTION AND HARVESTING OF MSCs

Human bone marrow derived MSCs were isolated with Institutional Review Board approval (University of Washington, Seattle, WA) from the femoral heads of patients undergoing total hip arthroplasty using a standard plastic adhesion protocol. Cells flushed from the bone marrow were pelleted and re-suspended in isolation medium [α-MEM + 1× Antibiotic–Antimycotic + 10% MSC qualified fetal bovine serum (FBS; all Gibco/Life Technologies, Grand Island, NY) + 1 ng/ml Fibroblast Growth Factor 2 (FGF-2, R&D Systems, Minneapolis, MN)], seeded into T150 flasks (Corning Incorporated) and incubated for 3–4 days at 37°C, 5% CO_2, then washed twice with phosphate buffered saline (PBS, pH 7.4), and incubated in fresh isolation medium. When colonies reached 80% confluence, cells were re-seeded at 1×10^6 cells/T150 flask in isolation medium. Medium was changed every 3–4 days until cells reached 80–90% confluency, at which time cells were either frozen or passaged.

CELL CULTURE AND OSTEOGENIC DIFFERENTIATION

For experiments, MSCs were expanded in growth medium (high glucose DMEM containing L-glutamine and sodium pyruvate + 1× Penicillin–Streptomycin + 10% MSC qualified FBS (all Gibco/Life Technologies), at 37°C, 5% CO_2. Growth medium was changed every

3–4 days until cells reached 70–80% confluence, at which time cells were seeded for experiments. For osteogenic differentiation MSCs were seeded at 20,000 cells/cm^2 and incubated in osteogenic medium (growth medium + 5 mM β-glycerophosphate, 50 μg/ml ascorbic acid, 10 nM dexamethasone, 10 nM 1,25-dihydroxyvitamin D_3; all Sigma–Aldrich, Saint Louis, MO) or growth medium as a control. Medium was changed every 3 days.

SUCROSE GRADIENT SUBCELLULAR FRACTIONATION

A previously published method was used for subcellular fractionation [Song et al., 1996a]. MSCs (1,140,000 cells at seeding) were homogenized in 2 ml of ice-cold 500 mM sodium carbonate pH 11.0 + 1:100 protease inhibitor cocktail, phosphatase inhibitor cocktail 2, and phosphatase inhibitor cocktail 3 (all Sigma–Aldrich), sonicated, mixed 1:1 with 90% sucrose in MBS buffer (50 mM MES, pH 6.5, 0.3 M NaCl), and placed at the bottom of a 14 × 89 mm^2 ultracentrifuge tube (Beckman, Palo Alto, CA). After 4 ml of 35% sucrose in 1:1 MBS: 500 mM sodium carbonate, followed by 4 ml of 5% sucrose in 1:1 MBS: 500 mM sodium carbonate were carefully layered on top, samples were centrifuged at 39,000 rpm in a Beckman XL-70 Ultracentrifuge (SW40Ti rotor) for 22 h. The contents of the centrifuge tubes were collected carefully in sequential 1 ml fractions from top to bottom.

ULTRASTRUCTURAL ANALYSIS OF SUCROSE GRADIENT FRACTIONS

Fractions 4, 5, and 6 from two sucrose gradients were combined and diluted 1:4 in 1:1 MBS: 500 mM sodium carbonate, then centrifuged at 39,000 rpm for 40 min. The supernatant was removed and replaced with ice-cold PBS + 10% sucrose. The isolated membrane preparation was either observed directly by cryo-electron microscopy or fixed, embedded, and sectioned for transmission electron microscopy (TEM). For the former, the membrane preparation was directly applied to glow-discharged Quantifoil grid (Quantifoil, Jena, Germany) for 1 min, then blotted and vitrified on a Vitrobot cryostation (FEI, Hillsboro, OR), and transferred to and observed on an FEI CM120 electron microscope operating at 120 keV. Micrographs were recorded on film at magnification of 38,000× at defocus values of 1.2–1.5 μm. For the latter, the membrane pellets were fixed in 2.5% paraformaldehyde (Electron Microscopy Sciences) + 2% glutaraldehyde (Sigma–Aldrich) in PBS for 2 h at room temperature, rinsed in 0.1 M cacodylate buffer (pH = 7.4), post-fixed in 1% OsO_4 + 0.8% potassium ferricyanide, rinsed, and dehydrated in an ascending ethanol series, and infiltrated and embedded with Epon-Araldite (Ted Pella, Redding, CA). Eighty-nanometer sections were cut on an ultramicrotome (Leica EM UC6), collected on copper slot grids, counterstained with uranyl acetate and lead citrate, and examined using an FEI Tecnai12 TEM operating at 120 keV.

ATPase ASSAY

Samples of each sucrose gradient fraction were pre-incubated with 1 mM of the Na^+/K^+-ATPase inhibitor ouabain (Tocris Bioscience, Redding, CA, 1 mM final concentration) or water (as a control) for 1 h on ice in the dark. Aliquots (100 μl) of each sample were assayed using a colorimetric ATPase assay (Innova Biosciences Ltd, Cambridge, Cambridgeshire, UK) according to the manufacturer's instructions, except NaCl and KCl were added to the manufacturer's substrate/buffer mix at final concentrations of 100 and 10 mM, respectively. Phosphate (Pi) concentration in each sample was determined by comparing to a Pi standard curve and enzyme activity calculated according to the manufacturer's instructions. Na^+/K^+-ATPase activity was estimated as the ouabin-inhibitable enzyme activity after subtraction of the activity in the presence of ouabain from the control.

WESTERN BLOTTING

Cells lysates were prepared in RIPA buffer + 1:100 protease inhibitor cocktail, phosphatase inhibitor cocktail 2, and phosphatase inhibitor cocktail 3 (all Sigma–Aldrich) and the protein concentration determined by BCA assay (Pierce Biotechnology, Rockford, IL). Equal volumes of protein (1 or 5 μg) were electrophoresed by SDS–PAGE in a 12% polyacrylamide gel and transferred to PVDF blots which were blocked in 5% milk or 5% bovine serum albumin (BSA, Sigma–Aldrich) in Tris buffered saline + 0.05% Tween 20 (TBST), then incubated overnight at 4°C with either rabbit anti-caveolin-1 (BD Biosciences, 1:5,000 in TBST + 2.5% milk); or mouse anti-GAPDH (Abcam, Cambridge, MA, 1:1,000 in TBST + 2.5% BSA). Secondary antibodies were Amersham ECL donkey anti-rabbit or sheep anti-mouse horseradish peroxidase (HRP)-linked IgG antibody (both GE Healthcare UK Limited, Little Chalfont, Buckinghamshire, UK). HRP activity was detected using Supersignal West Dura, Extended Duration Substrate (Pierce) and the chemiluminescent reaction visualized using a FOTO/Analyst® Fx CCD imaging system (Fotodyne Incorporated).

IMMUNOSTAINING

Cells were seeded onto glass coverslips at 10,000 cells/cm^2 and fixed 1 day later in 4% paraformaldehyde for 25 min at room temperature, permeabilized in 0.1% Triton X-100 (Sigma–Aldrich), blocked in 10% BSA in PBS for 1 h, and incubated with rabbit anti-human caveolin-1 (BD biosciences, 1:100) and Alexa Fluor® 594 Phalloidin (Life Technologies/Molecular Probes, Eugene, OR, 1:50) in 1% BSA in PBS, followed by Alexa Fluor® 647 conjugated chick anti-rabbit secondary antibody (Life Technologies/Molecular Probes) diluted 1:1,000 in 1% BSA in PBS. Stained cells were mounted on glass slides with VECTASHIELD® HardSet™ Mounting Medium with DAPI (Vector Laboratories, Inc., Burlingame, CA) and viewed on an Olympus Fluoview 500 confocal microscope (Olympus America, Inc., Center Valley, PA).

siRNA TRANSFECTION

MSCs were seeded at 20,000 cells/cm^2, incubated overnight, washed in serum free and antibiotic free high glucose DMEM and transfected with either 50 nM Human CAV1 ON-TARGET*plus* SMARTpool siRNA or 50 nM non-targeting control siRNA ON-TARGET*plus* non-targeting siRNA #2 (both Thermo Scientific/Dharmacon RNAi Technologies) using DharmaFECT1 Transfection Reagent (Thermo Scientific/Dharmacon RNAi Technologies, Lafayette, CO). DharmaFECT1 and each siRNA were prepared at 10× the final concentration used for transfection in serum-free and antibiotic-free high glucose DMEM and incubated for 5 min at room temperature. Each siRNA was then mixed 1:1 with the DharmaFECT1 and incubated for

20 min at room temperature. Each siRNA/DharmaFECT mix was then diluted 1:5 in antibiotic-free growth medium and added to washed MSCs at 0.13 ml/cm^2. The final volume of DharmaFECT used was 0.08 μl/cm^2. Twenty-four hours later medium was replaced with either fresh growth medium or osteogenic medium.

LENTIVIRAL shRNA TRANSDUCTION

Lentivirus expressing shRNA specific for caveolin-1 (oligo sequence: ccggccaccttcactgtgacgaaatctcgagatttcgtcacagtgaaggtggttttt) was provided by Dr R. W. Sobol at the University of Pittsburgh Cancer Institute (UPCI) Lentiviral Facility. Support for the UPCI Lentiviral Facility was provided to RWS by the Cancer Center Support Grant from the National Institutes of Health [P30 CA047904]. Medium was aspirated from MSCs at 50% confluence in a six-well plate and replaced with 2 ml/well lentivirus transduction solution [DMEM + 8 μg/ml polybrene (Sigma) + 1×10^6 virus particles] for 17 h at 32°C, 5% CO_2. MSCs were then returned to normal growth conditions (growth medium, 37°C, 5% CO_2). Puromycin (1 μg/ml, Sigma) was added to growth medium for selection of cells expressing the shRNA transgene 96 h post-transduction. Cells were then expanded in selection medium before osteogenesis experiments. Untransfected parental cells at a similar passage were used as a control for shRNA transduced cells.

RNA EXTRACTION AND REAL-TIME REVERSE TRANSCRIPTION (RT)-PCR

RNA was extracted using an RNeasy® plus mini kit (Qiagen Sciences, Valencia, CA) according to the manufacturer's instructions and quantified using a NanoDrop 2000c spectrophotometer (Thermo Scientific). RNA was reverse transcribed using SuperScript™ III First-Strand Synthesis SuperMix with Oligo(dT)$_{20}$ primers (Life Technologies, Carlsbad, CA) according to the manufacturer's instructions. cDNA (10 ng) was added to 12.5 μl SYBR® Green PCR master mix (Applied Biosystems, Foster City, CA) and 400 nM primers in a final volume of 25 μl for PCR on a 7900HT Fast Real-Time PCR machine (Applied Biosystems) using the following conditions: 94°C for 5 min, 40 cycles of: 94°C for 30 s, 65°C for 30 s, 72°C for 30 s, ending with 72°C for 5 min. Primer sequences were: (1) caveolin-1, modified from [Rodriguez et al., 2009], forward: 5′-ggg caa cat cta caa gcc caa caa-3′, reverse: 5′-ctg atg cac tga atc tca atc agg aa-3′; (2) Col1a2, from [Nesti et al., 2008], forward: 5′-ggc tcc tgc tcc tct tag cg-3′, reverse: 5′-cat ggt acc tga ggc cgt tc-3′; (3) GAPDH, from [Pricola et al., 2009], forward: 5′-caa ggc tga gaa cgg gaa gc-3′, reverse: 5′-agg ggg cag aga tga tga cc-3′; (4) Runx2 (designed by Dr. J. Taboas) forward 5′-caa cca cag aac cac aag tgc g-3′, reverse 5′-tgt ttg atg cca tag tcc ctc c-3′; (5) Bone Sialoprotein 2 (designed by Dr. L. Boyette), forward 5′-ggt ctc tgt ggt gcc ttc tg-3′, reverse 5′-tgc tac aac act ggg cta tgg-3′; and (6) Osteocalcin (designed by Dr. L. Boyette), forward 5′-atg aga gcc ctc aca ctc ctc-3′, reverse 5′-gcc gta gaa gcg ccg ata ggc-3′.

ALKALINE PHOSPHATASE ASSAY

Cultures in 24-well plates were washed in PBS, lysed in 150 μl 0.5% Triton X-100 in H_2O for 10 min at room temperature, then frozen and thawed twice. One hundred microliters of lysate was assayed spectrophotometrically using an equal volume of substrate buffer [(4 mg/ml 4-nitrophenyl phosphate (pNPP, Sigma–Aldrich), mixed 1:1 with AMP buffer (4.8% 2-amino-2-methyl-1-propanol (2-AMP, Sigma–Aldrich), 2 mM $MgCl_2$, pH 10.15)]. A_{415} values were used to calculate ALP activity and expressed as a function of DNA.

PICOGREEN ASSAY FOR DNA

DNA was quantified using Quant-iT™ PicoGreen® dsDNA reagent (Life Technologies/Molecular Probes), a fluorescent dsDNA stain (excitation 480 nm, emission 520 nm), according to the manufacturer's instructions. A Lambda phage DNA standard was used to quantify DNA from the fluorescence readings.

ALIZARIN RED STAINING

Cultures were washed in PBS, fixed in 60% isopropanol (diluted in tap H_2O), washed in tap H_2O, and stained with 2% Alizarin red S solution, pH 4.2, for calcium deposits (Rowley Biochemical Institute, Danvers, MA). Cultures were washed thoroughly with tap H_2O before scanning and imaging. Retained stain was solubilized using 0.5 ml 10% cetylpyridium chloride in 10 mM Na_2HPO_4 pH 7.0, at room temperature for 15 min and quantified spectrophotometrically at 570 nm and normalized to the DNA content measured in cell lysates of duplicate wells of each sample.

SUPERARRAY ANALYSIS

Superarrays used in this study were the RT^2 Profiler™ PCR Array Human Signal Transduction PathwayFinder and the RT^2 Profiler™ PCR Array Human Osteogenesis (SABiosciences/Qiagen, Frederick, MD). SuperArray analysis was performed according to the manufacturer's instructions using 560 ng RNA (for the Human Signal Transduction PathwayFinder array) or 280 ng RNA (for the Human Osteogenesis array) in the first step of reverse transcription using the RT^2 First Strand Kit (SABiosciences/Qiagen). Each array was performed using the manufacturer's recommended RT^2 SYBR Green/ROX PCR Master mix and PCR conditions. Data was analyzed using the RT^2 Profiler PCR Array Data Analysis web portal.

STATISTICAL ANALYSIS

All statistical analysis was performed using Student's 2-tailed *t*-test on two groups containing at least 3 samples each.

RESULTS

CAVEOLIN-1 IS EXPRESSED IN MSCs AND CO-FRACTIONATES WITH THE PLASMA MEMBRANE

Western blotting of total cell lysates from human MSCs with an anti-caveolin-1 antibody revealed a 22 kDa protein, which corresponds to the size of human caveolin-1 (data not shown). To determine if caveolin-1 is localized to lipid rafts, we fractionated MSC lysate using a sucrose gradient flotation method previously used by others [Song et al., 1996a] (Fig. 1). Caveolin-1 protein was detected in the 5th to 6th fractions (Fig. 1A), which contained 16% and 25% sucrose, with specific gravity of 1.08 and 1.12, respectively, and corresponded to fractions that should contain buoyant caveolae lipid rafts [Song et al., 1996a]. Note that some caveolin-1 protein was also detected in the bottom fractions of the gradient, probably

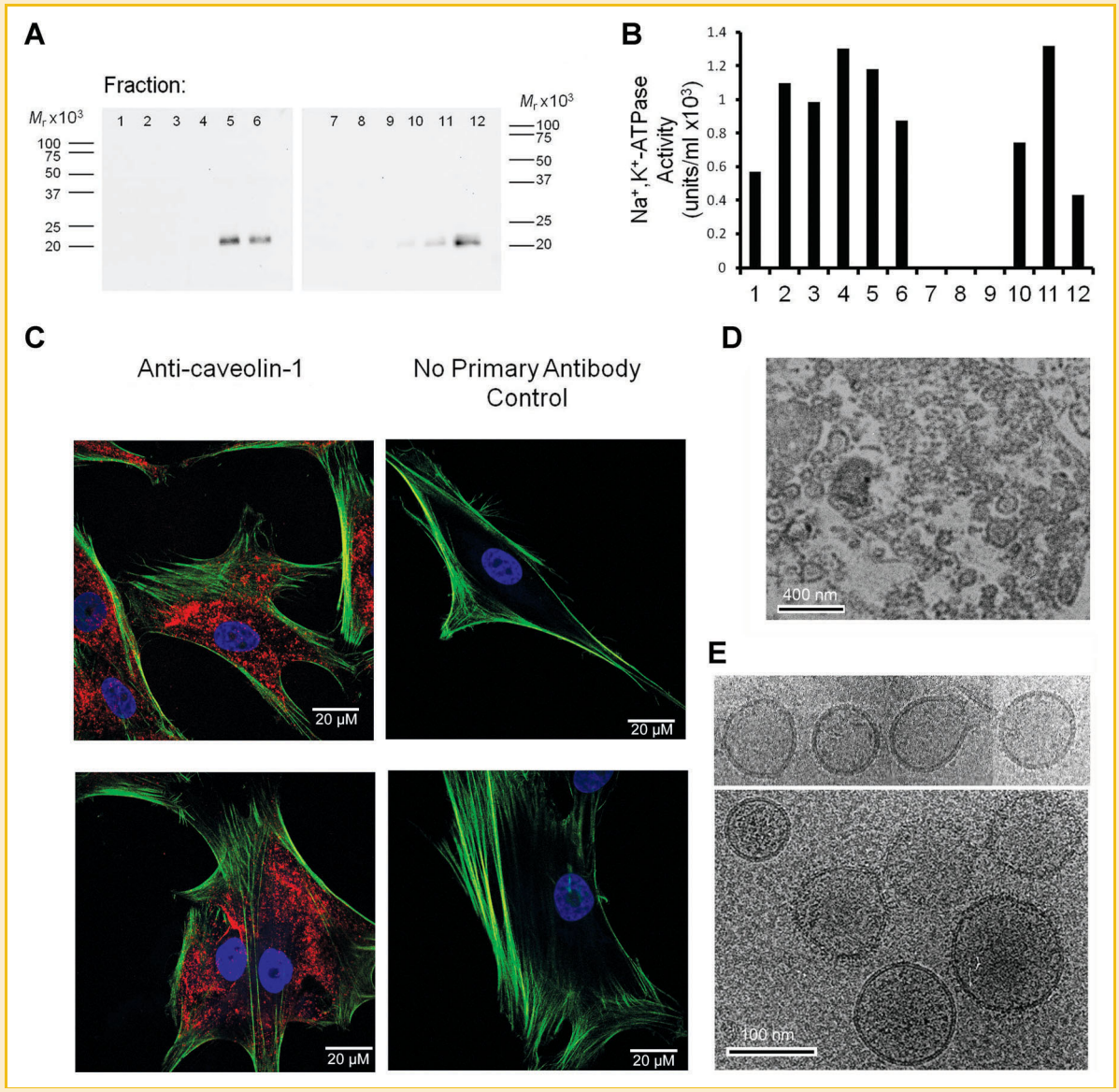

Fig. 1. Detection of caveolin-1 protein and morphology of fractionated caveolae in human MSCs. A: MSCs isolated from a female donor (66f) were lysed and fractionated by sucrose gradient ultracentrifugation. Fractions were immunoblotted for caveolin-1 (1 = top of the gradient, 12 = bottom of the gradient). Caveolin-1 was enriched in the buoyant density fractions 5 and 6 (16% sucrose, specific gravity 1.08, and 25% sucrose, specific gravity 1.12, respectively). These results are representative of 3/3 donors tested. Molecular weight markers are as indicated. B: The same fractions as in (A) were assayed for ATPase activity in the absence and presence of 1 mM ouabain, an inhibitor of the Na+/K+-ATPase activity that is located in the cell membrane. The ouabain-inhibitable ATPase activity in each fraction is presented. Na+/K+-ATPase activity was detected in buoyant density fractions (1–6) and in the bottom gradient fractions (10–12) that contain cell debris. C: MSCs were immunofluorescently stained with an antibody specific for caveolin-1 (red), with phalloidin filamentous actin staining (green) and DAPI nuclear staining (blue). Confocal images were taken at a 100× magnification. No staining was observed when the primary antibody was omitted. Bar = 20 μm. D,E: Ultrastructural morphology of caveolar lipid raft fractions isolated by density gradient centrifugation viewed by electron microscopy. Bar = 400 nm. D: Ultrathin section of epon-embedded membrane fraction; and (E) vitrified, cryo-preserved membrane fraction showing various morphologies of caveolae with an average diameter of <100 nm. Bar = 100 nm. [Color figure can be seen in the online version of this article, available at http://wileyonlinelibrary.com/journal/jcb]

representing caveolin-1 associated with a different compartment of the cell and/or with membrane fragments trapped within cell debris. To confirm that the upper sucrose gradient fractions contained the plasma membrane compartment of the cell, we measured the activity of Na^+/K^+-ATPase in the fractions using an ATPase assay in the presence and absence of ouabain, a Na^+/K^+-ATPase specific inhibitor. This assay confirmed that fractions 1–6 were enriched in Na^+/K^+-ATPase, a component of the plasma membrane (Fig. 1B). Therefore, caveolin-1 protein co-fractionated with buoyant plasma membrane components of MSC lysate on a sucrose density gradient. Again, some Na^+/K^+-ATPase activity was detected in the bottom fractions of the gradient, consistent with trapping of cell membrane in the cell debris. As described below, ultrastructural examination of the caveolin-1 enriched membrane fractions isolated by this method showed membrane bound vesicles with an average diameter similar to that reported for caveolae lipid rafts (see below).

CAVEOLIN-1 LOCALIZATION IN MSCs

To further investigate the localization of caveolin-1 in MSCs we performed immunofluorescence staining of MSCs with the anti-caveolin-1 antibody and observed the staining pattern by confocal microscopy. Typical punctate staining was observed, suggestive of caveolin-1 localization to caveolae (Fig. 1C). No staining was observed in controls that omitted the primary antibody. We also stained MSCs with another anti-caveolin-1 antibody (from a different supplier) and observed a similar pattern (data not shown). The pattern of caveolin-1 immunostaining in MSCs was very similar to that in the endothelial cells (data not shown) which are known to have caveolae and express caveolin-1 [Griffoni et al., 2000].

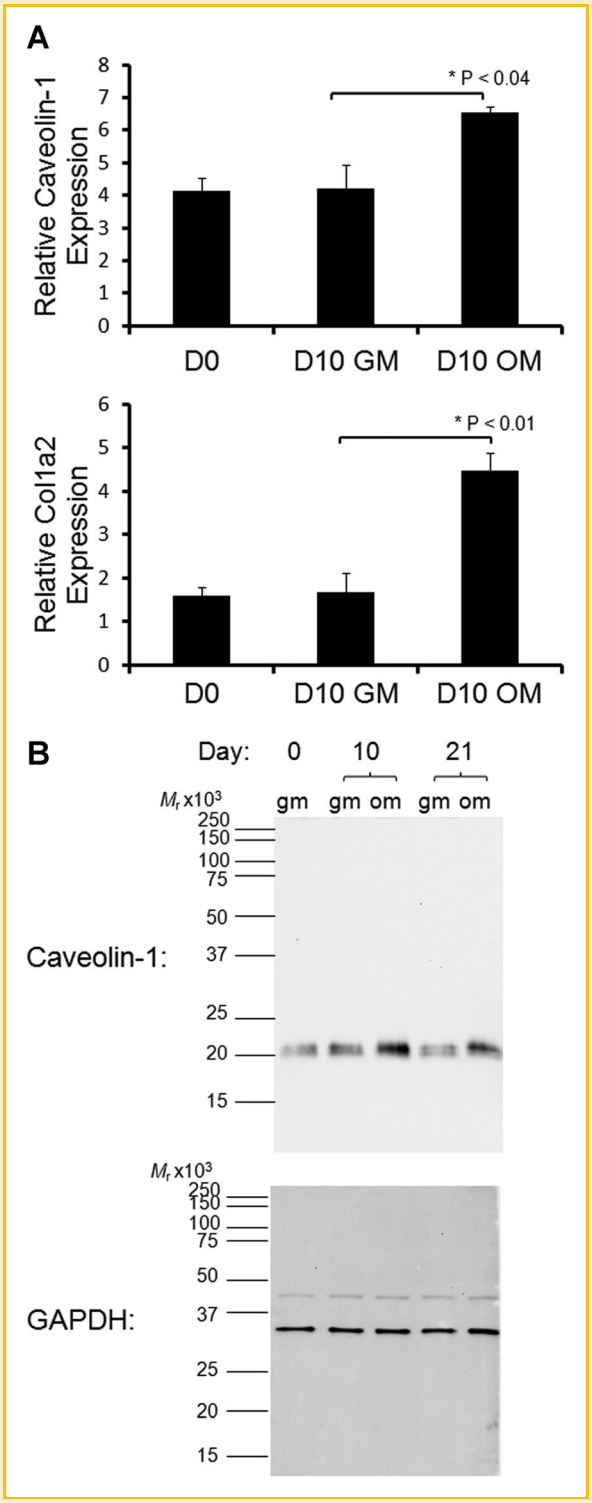

ULTRASTRUCTURAL OBSERVATION OF CAVEOLAE IN ISOLATED MEMBRANE FRACTIONS

As others have observed an increased bone volume in caveolin-1 knockout mice [Rubin et al., 2007], we next investigated the expression of caveolin-1 and presence of caveolae in MSCs induced to undergo osteogenic differentiation. Caveolin-1 protein was detected in similar density gradient cell membrane fractions of osteogenically differentiated MSCs as control MSCs (data not shown). TEM of ultrathin epon sections revealed the abundance of small membrane bound vesicles in the caveolin-1 enriched fractions (Fig. 1D), and observation of vitrified, cryo-preserved samples showed the fine structure of these vesicles with an average diameter of $\leq$100 nm (Fig. 1E), corresponding to the reported size of caveolae. Similar dimension plasma membrane invaginations, morphologically similar to caveolae, were also detected by TEM in MSCs induced to undergo osteogenic differentiation (not shown).

CAVEOLIN-1 EXPRESSION INCREASES IN OSTEOGENICALLY INDUCED MSCs

MSCs grown in osteogenic medium showed increased expression of caveolin-1 mRNA and protein compared to control MSCs, suggesting that caveolin-1 may be involved in osteogenic differentiation (Fig. 2). Upregulation of caveolin-1 mRNA was evident at Day 10 (Fig. 2A), concomitant with that of Col1a2 mRNA (Fig. 2A). Upregulation of caveolin-1 mRNA at Day 10 of osteogenesis was observed in three out of three donor MSC populations tested. Increased levels of caveolin-1 protein were also evident at Day 10 and at Day 21 of osteogenic differentiation (Fig. 2B). Furthermore, upregulation of caveolin-1 mRNA expression was often seen as early as Day 1 of osteogenesis in six donor MSC populations studied in subsequent experiments (Fig. 3A and data not shown).

Fig. 2. Caveolin-1 expression increases in MSCs induced to osteogenically differentiate. A: Expression of caveolin-1 (top panel) and Col1a2 (bottom panel) mRNA was measured by two-step real time RT-PCR and normalized to the housekeeping gene GAPDH in RNA samples from MSCs (donor 65f) seeded in regular growth medium before addition of osteogenic medium (Day 0, D0) or grown for 10 days in regular growth medium (D10, GM) or osteogenic medium (D10, OM). Values represent the mean $\pm$ SEM (three wells). After 10 days of osteogenic differentiation expression of both caveolin-1 and Col1a2 mRNA were upregulated. Upregulation of caveolin-1 mRNA in osteogenic medium was seen in 3/3 donors. B: Cell lysates harvested from MSCs from the same experiment as in (A) at day 0, 10, and 21 were immunoblotted with an antibody specific for caveolin-1 (BD Biosciences) or for GAPDH (gm, growth medium; om, osteogenic medium). Molecular weight standards are as indicated. Expression of caveolin-1 protein was elevated in MSCs grown in osteogenic medium while the expression of GAPDH did not change.

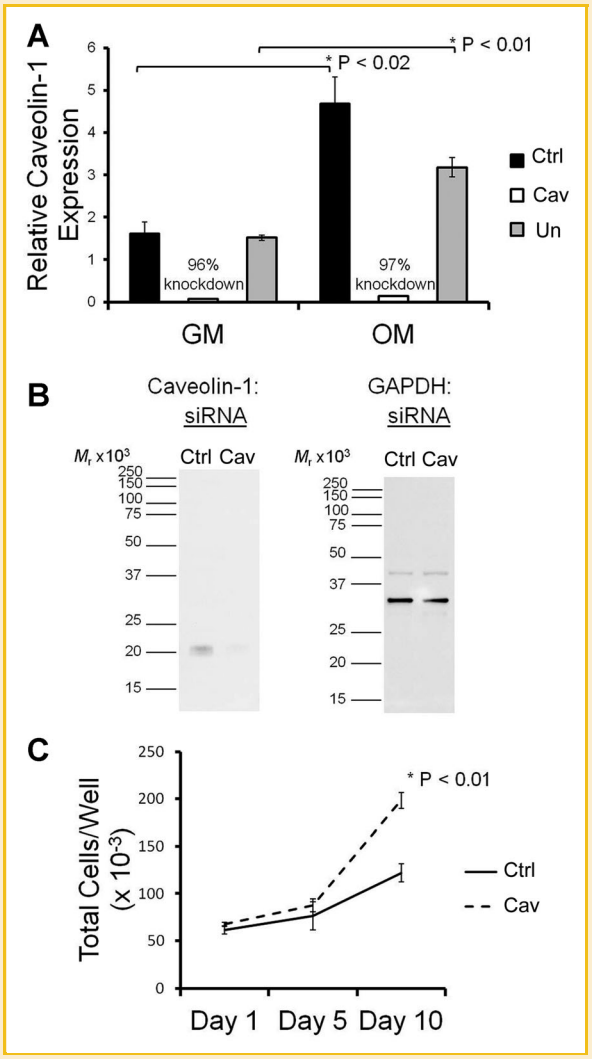

Fig. 3. Caveolin-1 knockdown in MSCs. MSCs were transfected with a non-targeting control siRNA (Ctrl) or caveolin-1 siRNA (Cav). A: Caveolin-1 mRNA expression was measured in MSCs transfected with siRNA (Ctrl, Cav) or left untransfected (Un) then incubated in growth medium (GM) or osteogenic medium (OM). RNA samples were harvested 48 h post transfection and 24 h post addition of growth medium or osteogenic medium. Caveolin-1 siRNA knocked-down caveolin-1 mRNA expression by at least 93% in all samples compared to controls at this time point in each donor/experiment. Results from donor 50m are presented and show that caveolin-1 mRNA expression was reduced by 96% and 97% in MSCs transfected with caveolin-1 siRNA and incubated in growth medium and osteogenic medium, respectively. Also note that caveolin-1 expression was significantly upregulated by osteogenic medium in both control siRNA transfected cells and untransfected cells. B: Protein samples from siRNA transfected MSCs (donor 50m) incubated in growth medium as described in (A) were immunoblotted for caveolin-1 or for GAPDH. Transfection with caveolin-1 siRNA greatly reduced expression of caveolin-1 protein. C: MSCs (donor 60f) transfected with siRNA were grown in growth medium for 1, 5, and 10 days. At each time point cells were counted. By day10, proliferation was significantly greater in cells transfected with caveolin-1 siRNA suggesting a reduction in caveolin-1 expression enhances cell proliferation. Values are the mean ± SEM (three wells). Caveolin-1 siRNA significantly enhanced cell proliferation in 3/5 donor MSC populations tested.

CAVEOLIN-1 EXPRESSION CAN BE KNOCKED-DOWN IN MSCs USING siRNA

To determine if caveolin-1 has a role in MSC osteogenesis, we examined the effect of caveolin-1 knockdown using siRNA. The efficiency of the siRNA mediated knockdown was confirmed by real-time RT-PCR and Western blotting (Fig. 3): caveolin-1 mRNA was knocked-down by over 90% at 48 h post-transfection (example in Fig. 3A), with a concomitant decrease in caveolin-1 protein level (Fig. 3B).

KNOCKDOWN IN CAVEOLIN-1 EXPRESSION INCREASES MSC PROLIFERATION

As caveolin-1 knockdown has been reported to increase proliferation in other cell types [Galbiati et al., 1998], we tested whether caveolin-1 knockdown had this biological effect on MSCs. We observed that transfection with caveolin-1 siRNA resulted in a significant increase in cell proliferation after 10 days of culture in normal growth medium. This effect was seen in three out of three female donor MSC populations tested (example shown in Fig. 3C), and of the two male donor MSC populations tested, there was a trend increase in proliferation in one that did not reach statistical significance ($P = 0.06$).

KNOCKDOWN IN CAVEOLIN-1 EXPRESSION INCREASES ALKALINE PHOSPHATASE ACTIVITY IN MSCs INDUCED TO UNDERGO OSTEOGENESIS

We next tested the effect of caveolin-1 knockdown on MSC osteogenesis (Fig. 4). When caveolin-1 expression was knocked-down, we observed an enhancement in alkaline phosphatase (ALP) activity after 4-day culture in osteogenic medium compared to transfection with a non-targeting control siRNA. This result was seen in four out of four female donor MSC populations tested and three out of three male donor MSC populations tested (examples shown in Fig. 4A and Fig. S1 in Supplementary Material). These results suggested that reduced caveolin-1 expression could enhance the early phase of MSC osteogenesis.

KNOCKDOWN IN CAVEOLIN-1 EXPRESSION INCREASES ALIZARIN RED STAINING IN SOME OSTEOGENICALLY INDUCED MSCs

After 21 days of osteogenic induction, knockdown of caveolin-1 expression was associated with increased Alizarin red staining in two MSC donor populations tested (50m and 60f). The results from 50m are shown in Figure 4B,C. Given our previous observation of enhanced MSC proliferation with caveolin-1 knockdown, Alizarin red staining was quantified spectrophotometrically and normalized to DNA content in duplicate wells. The results confirmed the increased matrix mineralization upon caveolin-1 knockdown (Fig. 4D). In 60f, enhanced Alizarin red staining was observed as early as Day 10 (refer to Fig. S1B–D in Supplementary Material). However, in the five other MSC populations tested, Alizarin red staining was not enhanced in caveolin-1 siRNA transfected cells (an example from a female donor MSC population, 49f, is shown in Fig. 4E).

As enhanced Alizarin red staining was only observed in two out of seven MSC populations, we hypothesized that this could be due to reduced and variable knockdown of caveolin-1 expression by the

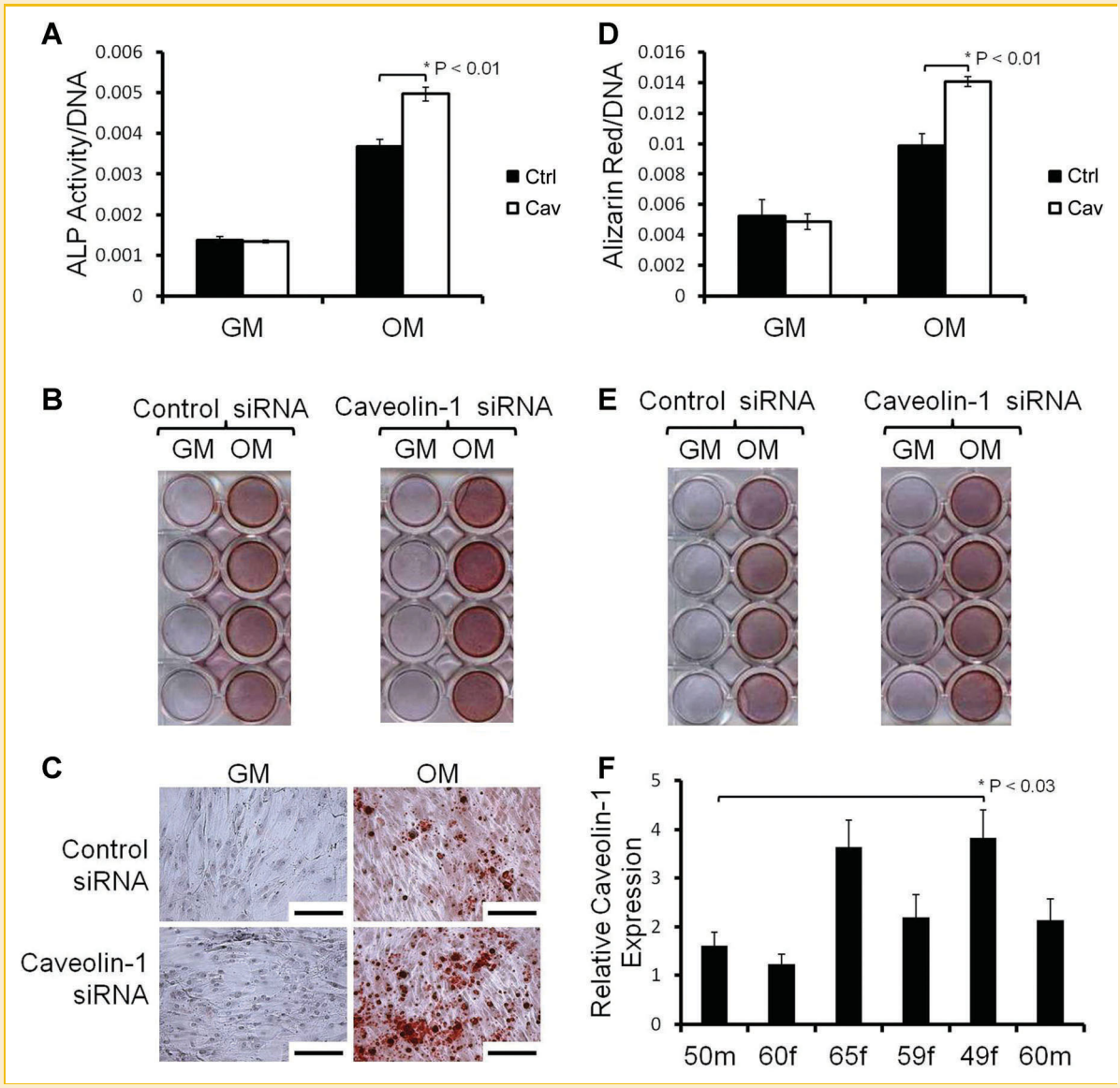

Fig. 4. Effect of caveolin-1 knockdown on MSC osteogenic differentiation. MSCs were transfected with a non-targeting control siRNA (Ctrl) or with caveolin-1 siRNA (Cav) then incubated in growth medium (GM) or osteogenic medium (OM). A: ALP activity at culture Day 4 normalized to DNA content (donor 50m). Values are the mean ± SEM (four wells). ALP activity was significantly enhanced in osteogenic cultures transfected with caveolin-1 siRNA. B–F: Alizarin red staining of matrix mineralization at culture Day 21 (four replicate wells). Donor 50m cultures showed enhanced Alizarin red staining in whole cells (B) and low magnification bright field optics (C) upon caveolin-1 knockdown. Bar = 200 μm. (D) Quantification of Alizarin red stain in each well in (B) was normalized to DNA measured in duplicate wells. Values are the mean ± SEM (four wells). There was significantly more Alizarin red stain/DNA harvested from osteogenic cultures transfected with caveolin-1 siRNA. E: Donor 49f cultures did not show enhanced Alizarin red staining when cells were transfected with caveolin-1 siRNA. F: Basal caveolin-1 mRNA expression measured by real-time RT-PCR in day 1 control siRNA growth medium samples from various donor MSCs used in this study. Donor 49f showed significantly greater basal expression of caveolin-1 mRNA than 50 m. Caveolin-1 expression was normalized to GAPDH, and values are mean ± SEM (three wells). [Color figure can be seen in the online version of this article, available at http://wileyonlinelibrary.com/journal/jcb]

end of the 21-day culture period. Interestingly, 50m and 60f had the lowest basal expression of caveolin-1 mRNA in control samples at the beginning of the osteogenesis time course (Fig. 4F). We measured expression of caveolin-1 mRNA in biological duplicates on Day 21 of osteogenesis in 50m and 49f (Fig. S2 in Supplementary Material). Knockdown of caveolin-1 mRNA was 36% in the former and only 6% in the latter (see Fig. S2A,B in Supplementary Material). As we had anticipated problems with the longevity of caveolin-1 knockdown, we transfected cells from these two donors with caveolin-1 siRNA a second time at the beginning of the second week and a third time at the beginning of the third week of osteogenesis in parallel cultures in the same experiment (Fig. 5). The extra transfections were not toxic to the cell cultures and resulted in greater caveolin-1 knockdown at the end of the 21-day time course. In both cell populations, caveolin-1 knockdown was 87% in osteogenic medium according to measurements in biological duplicates (see Fig. S2C,D in Supplementary Material). In cells from 50m, in which enhanced Alizarin red staining occurred with

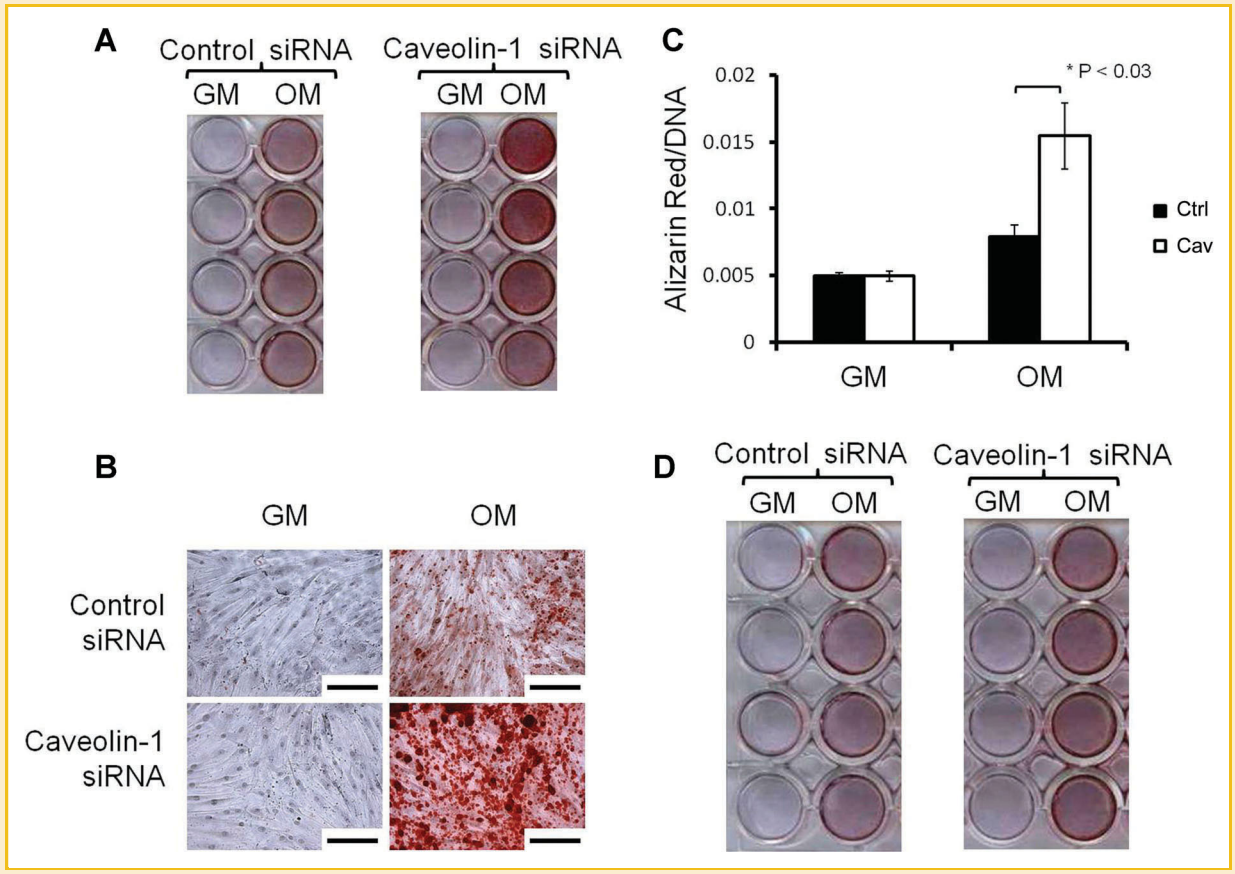

Fig. 5. Effect of triple transfection of caveolin-1 siRNA on MSC osteogenic differentiation. In a similar set up as in Figure 4, quadruplicate wells of cells from donors 50m and 49f were transfected two additional times, on culture Day 6 and Day 13. A,B: Donor 50m cultures exhibited even greater enhanced Alizarin red staining in caveolin-1 siRNA transfected cells compared to cells transfected once (Fig. 4B): (A) Whole cell view and (B) low magnification bright field view. Bar = 200 μm. C: Quantification of Alizarin red stain in each well in (A) normalized to DNA; values are the mean ± SEM (four wells) and show Alizarin red staining was significantly greater in osteogenic cultures transfected with caveolin-1 siRNA. D: Additional siRNA transfections appeared not to cause an enhancement of Alizarin red staining in cells from donor 49f. [Color figure can be seen in the online version of this article, available at http://wileyonlinelibrary.com/journal/jcb]

one caveolin-1 siRNA transfection, the enhancement in Alizarin red staining was even greater when cells were transfected two more times during the course of osteogenesis, suggesting this was a genuine effect of caveolin-1 knockdown (Fig. 5A–C). However, in 49f the effects of additional siRNA transfections were insignificant (Fig. 5D).

As another approach to achieve stable knockdown, we infected MSCs with a lentiviral construct harboring shRNA targeted against caveolin-1. Infection of MSCs with shRNA specific for caveolin-1 resulted in a reduction in caveolin-1 mRNA expression and enhanced ALP activity and Alizarin red staining when cells were incubated in osteogenic medium, in agreement with the siRNA findings (see Fig. S3 in Supplementary Material). However, uninfected cells had to be used as a control in this experiment, because cells infected with a scrambled shRNA control senesced in culture. Meanwhile, the caveolin-1 shRNA infected cells had a high proliferative rate, in keeping with caveolin-1 negatively regulating MSC proliferation. Furthermore, although it was possible to normalize ALP activity to DNA content in Day 4 osteogenisis samples, it was not possible to extract DNA from the highly mineralized caveolin-1 shRNA cultures at Day 21 of osteogenesis. Therefore, another caveat of these results is our inability to normalize Alizarin red staining to DNA content.

EFFECT OF CAVEOLIN-1 KNOCKDOWN ON OSTEOGENIC GENE EXPRESSION IN MSCs

We performed an RT-PCR based SuperArray to assess the expression of 84 different osteogenic genes in MSCs transfected with caveolin-1 siRNA or control siRNA and incubated in control growth medium or osteogenic medium for 10 days (Fig. 6). For this large analysis of gene expression, we used MSCs pooled from four different donor sources. The expression of caveolin-1 was still significantly decreased in caveolin-1 siRNA transfected cells at this time point (see Fig. S4 in Supplementary Material). There was a trend increase in expression of osteogenic genes in MSCs transfected with caveolin-1 siRNA and incubated in osteogenic medium compared to MSCs transfected with control siRNA and incubated in osteogenic medium (Fig. 6A and Fig. S4B in Supplementary Material). While *COL10A1* appeared as the most upregulated osteogenic gene in cells transfected with caveolin-1 siRNA, there was no statistically significant difference between control siRNA and caveolin-1 siRNA transfected cells (see Fig. S4A in Supplementary Material). In

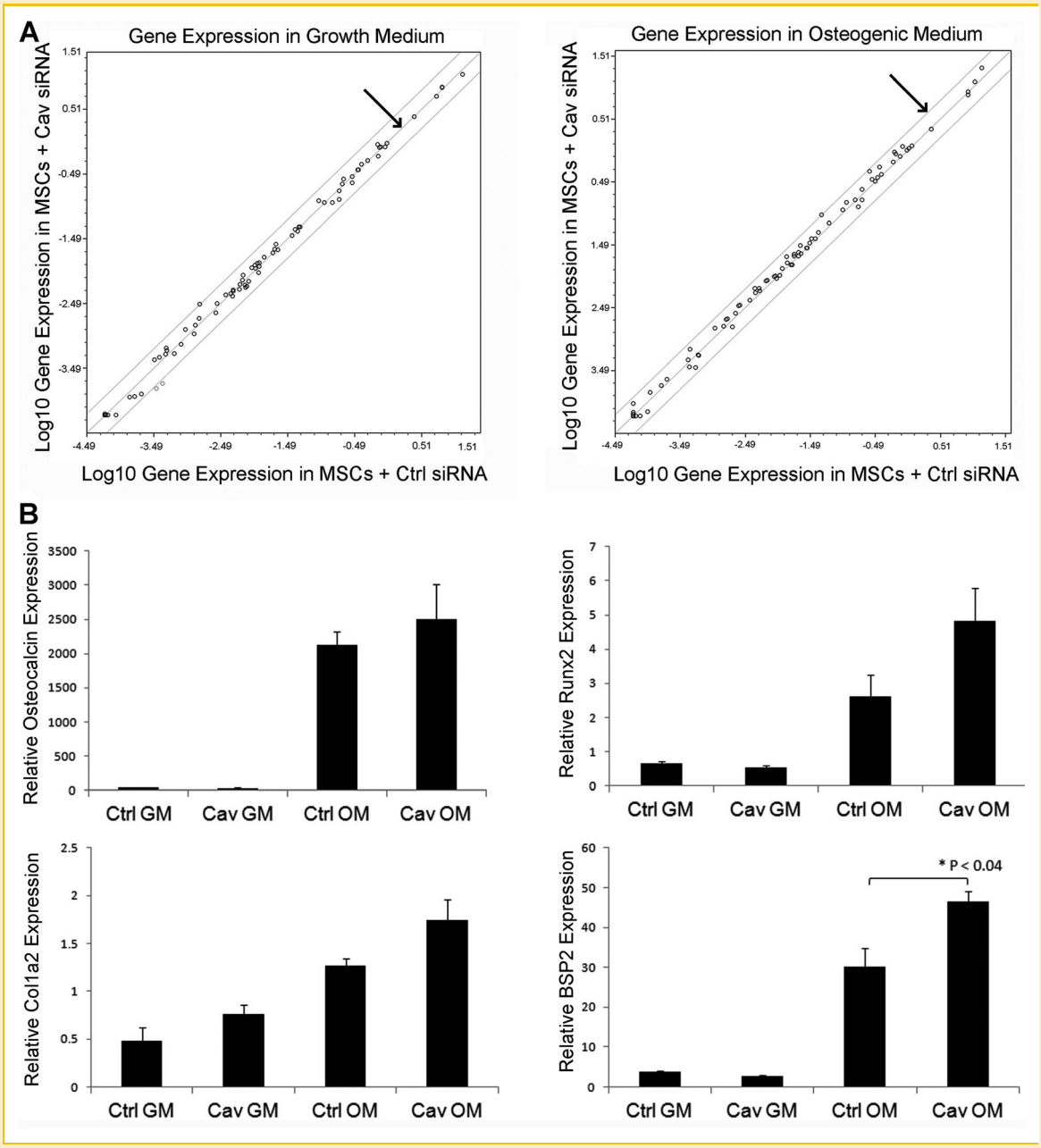

Fig. 6. Expression of osteogenic genes in MSCs treated with control and caveolin-1 siRNA. MSCs from four donor populations (59f, 49f, 50m, and 65f) at the same passage were pooled and transfected with either control siRNA (Ctrl) or caveolin-1 siRNA (Cav). Twenty-four hours after transfection cells were incubated in growth medium (GM) or osteogenic medium (OM) for 10 days and the RNA harvested for gene expression analysis. A: A qPCR array was performed for 84 different osteogenic genes. Scatter plots are presented comparing the gene expression profiles between caveolin-1 siRNA transfected MSCs and control siRNA transfected MSCs incubated in growth medium (left panel) or osteogenic medium (right panel). Lines delineate twofold differential expression. Although there were no significant differences in gene expression between caveolin-1 and control siRNA transfected cells, there was a trend up-regulation in many osteogenic genes in caveolin-1 siRNA transfected cells grown in osteogenic medium (see arrow right panel) compared to control siRNA transfected cells. When cells were grown in growth medium, gene expression in the caveolin-1 siRNA transfected cells differed slightly above and below expression in control siRNA transfected cells (see arrow left panel) with no general trend towards up or down regulation. B: Standard RT-PCR of the same samples for osteogenic genes produced similar results. Osteocalcin, Col2a1, Runx2, and bone sialoprotein 2 (BSP2) expression were each upregulated in cells grown in osteogenic medium (OM) compared to cells grown in growth medium (GM). There was a trend upregulation in expression of these genes in cells transfected with caveolin-1 siRNA and incubated in osteogenic medium. In the case of BSP2 expression this trend reached statistical significance. Values are the mean ± SEM (three wells).

addition to the array, we assessed the expression of osteocalcin, Runx2, Col1a2, and bone sialoprotein 2 (BSP2) mRNA by standard real-time PCR in the same samples. Similar to the array data, there was a trend upregulation in the expression of each of these osteogenic genes in MSCs transfected with caveolin-1 siRNA and incubated in osteogenic medium compared to controls (Fig. 6B). In the case of BSP2, this upregulation reached statistical significance ($P < 0.04$, Fig. 6B).

POTENTIAL CELL SIGNALING PATHWAYS MODULATED BY CAVEOLIN-1 KNOCKDOWN IN MSCs

To assess the effect of caveolin-1 knockdown on signaling pathways in MSCs undergoing osteogenic induction, we performed an RT-PCR based SuperArray gene expression analysis of genes downstream of major cell signaling pathways in MSCs transfected with caveolin-1 siRNA or control siRNA and incubated in osteogenic medium. RNA was harvested from cells 48 h post-siRNA transfection and 24 h post-addition of osteogenic medium. The PCR array was performed on RNA from the donors that showed enhanced Alizarin red staining (50m, 60f) and RNA pooled from donors 65f, 60m, and 59f (pool), that showed enhanced ALP activity but not enhanced Alizarin red staining. Analysis of the data from all three RNA samples (50m, 60f, and the pooled RNA) revealed no significant differences in gene expression profiles between the control siRNA samples and the caveolin-1 siRNA samples (data not shown). However, the lack of significant gene expression changes appeared to be related to large variations in gene expression among the different samples tested. When changes in gene expression in individual caveolin-1 knockdown samples versus control samples was examined, it was apparent that some changes in gene expression had occurred in different genes in different samples (Fig. 7). Of particular note, expression of growth regulation by estrogen in breast cancer 1 (*GREB1*), a target of estrogen signaling, was downregulated in the caveolin-1 siRNA samples from 60f and the pool. Meanwhile, expression of Kallikrein-related peptidase 2 (*KLK2*), a target of androgen signaling, was upregulated in the caveolin-1 siRNA samples from 50m and the pool. These preliminary findings suggest that hormone signaling pathways may be altered in MSCs with reduced caveolin-1 expression incubated in osteogenic medium.

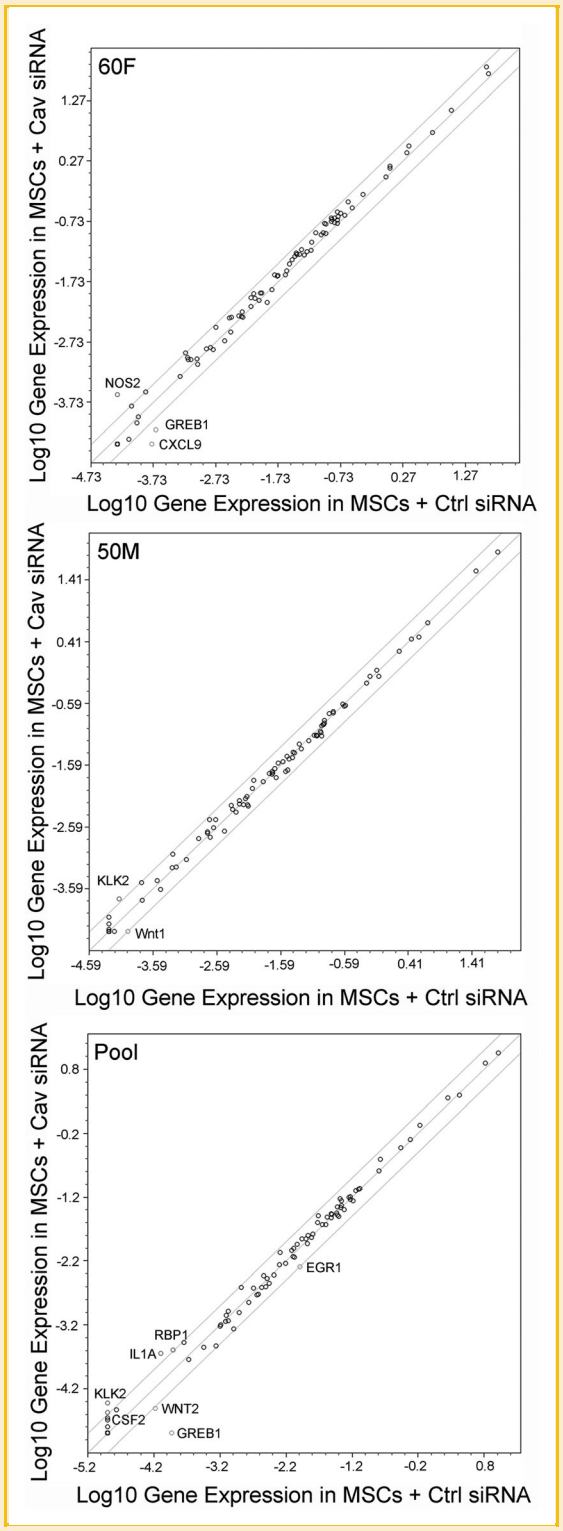

Fig. 7. Expression of genes immediately downstream of signaling pathways in MSCs treated with control and caveolin-1 siRNA. MSCs were transfected with control (Ctrl) or caveolin-1 (Cav) siRNA and then stimulated with osteogenic medium 24 h later. RNA was extracted 48 h post-siRNA transfection and 24 h post-addition of osteogenic medium, reverse transcribed and a qPCR array performed to assess the expression of genes known to be downstream of various cell signaling pathways. Scatter plots comparing gene expression in caveolin-1 and control siRNA transfected MSCs from donor 60f (top panel, 60F), 50m (middle panel, 50M) and 65f, 60m, and 59f (bottom panel, Pool) are presented. Genes with over a twofold differential expression (indicated by lines) are labeled. GREB1 expression was downregulated in caveolin-1 siRNA transfected cells from donor 60f and the pool (65f, 60m, 59f). KLK2 expression was upregulated in caveolin-1 siRNA transfected cells from donor 50m and the pool. These were the only two genes that showed more than twofold regulation in more than one sample tested.

DISCUSSION

In this study, we have demonstrated the expression of caveolin-1 and its presence in buoyant membrane fractions in human bone marrow derived MSCs. Caveolin-1 mRNA was detected by real-time RT-PCR and protein was detected by Western blotting and confocal immunofluorescence microscopy. Subcellular fractionation results strongly suggest the localization of caveolin-1 protein to caveolae, because caveolin-1 protein was present in the buoyant density lipid raft membrane fraction of MSCs. In agreement with this, immunofluorescence staining of caveolin-1 in MSCs revealed a punctate distribution. Ultrastructural observations also revealed the presence of caveolae-like membrane bound vesicles of ~100 nm

dimension in the fractionated lipid raft preparation from osteogenically differentiated MSCs. To investigate the role of caveolin-1 in MSC biology, we assessed the expression of caveolin-1 and the effect of knockdown of caveolin-1 expression during MSC osteogenic differentiation. To this end we discovered that caveolin-1 expression increases in MSCs undergoing osteogenesis and knockdown of caveolin-1 expression enhances MSC osteogenesis.

Our detection of caveolin-1 expression in human MSCs is in agreement with those of others who have previously shown the presence of caveolin-1 protein in total cell lysates of MSCs isolated from human bone marrow [Park et al., 2005]. We have extended this finding by demonstrating the immunolocalization of caveolin-1 in MSCs, and by showing enrichment of caveolin-1 protein in the isolated lipid raft membrane fraction of MSCs, which consists of abundant ~100 nm diameter, caveolae-like membrane vesicles. We also observed caveolin-1 in the bottom fractions of fractionated MSC lysate. This may be caveolin-1 present in debris and/or in a different compartment of the cell. It is known that caveolin-1 cycles between the cell membrane, endoplasmic reticulum, and Golgi apparatus [Conrad et al., 1995].

We observed that caveolin-1 expression increases from Day 1 of MSC osteogenesis onwards. This agrees with previous findings that caveolin-1 is highly expressed in terminally differentiated cells of mesenchymal lineages, including primary human osteoblasts and murine osteoblastic MC3T3 cells [Solomon et al., 2000; Lofthouse et al., 2001], primary rat adipocytes [Kandror et al., 1995], and rat and human articular chondrocytes [Schwab et al., 1999, 2000]. To probe the role of caveolin-1 in MSC osteogenesis, we knocked-down caveolin-1 expression in MSCs before osteogenic induction. Knockdown of caveolin-1 expression was confirmed at the mRNA and protein level and had the predicted effect of increasing cell proliferation. Elevated levels of caveolin-1 protein are found in human MSCs cultured to senescence (passage 26 compared to passage 6), suggesting that caveolin-1 expression is inversely related to proliferative rate in these cells [Park et al., 2005]. Our results agree with this as well as with studies in other cell types that show caveolin-1 negatively regulates cell proliferation [Engelman et al., 1997; Galbiati et al., 1998; Galbiati et al., 2001], and observations of increased populations of cells expressing stem cell markers in the gut, mammary gland, and brain of the caveolin-1 knockout mouse [Li et al., 2005; Sotgia et al., 2005; Jasmin et al., 2009]. Furthermore, over a similar culture period (10 days) to our study, MEFs isolated from the caveolin-1 knockout mouse have a twofold higher proliferative rate than wild type MEFs [Razani et al., 2001] and bone marrow derived MSCs from caveolin-1 knockout mice have also been noted to proliferate more rapidly than wild type cells [Case et al., 2010].

Upon osteogenic induction, MSCs transfected with caveolin-1 siRNA showed enhanced differentiation compared to controls, with greater ALP activity after 4 days of culture in osteogenic medium. MSCs transfected with caveolin-1 siRNA also showed a trend of increased expression of osteogenic genes at Day 10 of osteogenesis, and this was statistically significant for BSP2 expression. In two populations of MSCs studied, Alizarin red staining was also greater in MSCs transfected with caveolin-1 siRNA than in controls after longer culture in osteogenic medium, suggesting that reduced caveolin-1 expression enhances matrix mineralization during osteogenesis. However, it is noteworthy that enhanced Alizarin red staining in caveolin-1 siRNA transfected cells was not reproduced in all populations of MSCs studied. This could be the result of intrinsic variability among different subjects and variable levels of caveolin-1 expression at later stages of osteogenic differentiation. Repeated siRNA transfections led to a greater enhancement in Alizarin red staining in cells from one donor that had shown enhancement with one transfection, but still did not lead to significant enhancement of Alizarin red staining in cells of the another donor. The caveolin-1 expression level could have been too high at Day 21 in cells from the second donor to effect matrix mineralization. Perhaps caveolin-1 expression in this donor also recovered more between siRNA transfections. Preliminary experiments with shRNA suggest that stable knockdown of caveolin-1 expression greatly increases matrix mineralization of MSCs in osteogenic culture (see Supplementary Material Fig. S3). However, this data is presented with caveats: it was difficult to extract DNA from the highly mineralized cultures and thus solubilize and normalize the Alizarin red staining to DNA. Furthermore, uninfected parental cells had to be used as a control, because cells infected with a control scrambled shRNA senesced in culture while the caveolin-1 shRNA infected cells were highly proliferative.

The enhancement of MSC osteogenesis we observed with caveolin-1 knockdown is in agreement with observations made with the caveolin-1 null mice [Rubin et al., 2007]. These animals show increased bone volume and bone formation rate during postnatal growth, and in vitro studies with their bone marrow MSCs suggested this increase in bone volume is due to an increased propensity to form bone cells with a greater tendency to mineralize in response to osteogenic supplements, rather than a decreased tendency to form osteoclasts [Rubin et al., 2007]. In addition, caveolin-1 knockdown in CIMC-4 pre-osteoblast cells increases ALP activity [Rubin et al., 2007]. These findings agree with our human MSC results. However, it should be noted that another study reported that bone marrow MSCs from caveolin-1 null mice failed to mineralize in vitro and did not express bone sialoprotein [Case et al., 2010]. These contrasting results could be due to a difference in cell culture and composition of the osteogenic medium used. Most notably, Case et al. [2010] seeded cells on collagen type I and the concentration of β-glycerophosphate used was lower than that used here and by Rubin et al. [2007].

That reduced caveolin-1 expression causes enhanced osteogenesis and that caveolin-1 expression increases with osteogenesis may initially seem contradictory. However, caveolin-1 expression may increase during osteogenesis as a negative feedback to stabilize the differentiated phenotype and to reduce cell growth and cell responsiveness to differentiation stimuli. Interestingly, overexpression of caveolin-1 in human MSCs inhibits their adipogenesis [Park et al., 2005], consistent with caveolin-1 negatively regulating MSC differentiation. Mechanistically, a higher level of caveolin-1 in the differentiating cell could result in more caveolae formation and hence more compartmentalization of signaling proteins in caveolae, thus altering the cell's capacity to respond to growth and differentiation stimuli. Others have indeed suggested that caveolin-1 may inhibit continuous signals stimulating osteoblast

differentiation and help maintain cells in a less differentiated state [Rubin et al., 2007]. Also, others have already suggested that caveolin-1 expression plays a key role during differentiation, citing increased caveolin-1 expression upon the differentiation of many other cell types [Sotgia et al., 2005 and references therein].

Given the hypothesis outlined above, we would expect that our knockdown of caveolin-1 expression in MSCs enhances cell signaling in response to osteogenic stimuli. In particular, β-catenin or BMP signaling could be affected, because caveolin-1 is known to regulate these pro-osteogenic pathways [Galbiati et al., 2000; Lu et al., 2003; Nohe et al., 2005; Torres et al., 2007; Wertz and Bauer, 2008; Rodriguez et al., 2009; Mo et al., 2010; Du et al., 2011]. However, in global analysis of RNA derived from five subjects (two individual RNA samples and one sample of RNA pooled from three individuals), we did not observe any significant changes in the expression of the candidate genes in caveolin-1 knockdown samples assayed by SuperArrays. Downregulated expression of *GREB1* in two caveolin-1 knockdown samples and upregulated *KLK2* expression in two caveolin-1 knockdown samples suggests that caveolin-1 knockdown may affect estrogen and androgen signaling in MSCs in osteogenic medium. Whether this is related to the enhanced osteogenesis observed in caveolin-1 depleted cells requires further investigation. Interestingly, caveolin-1 has been reported to mediate 17β-estradiol induced mouse ES cell proliferation [Park et al., 2009]. Assessment of gene expression at different time points may help to identify signaling pathways altered by caveolin-1 knockdown in further studies. Furthermore, each population of MSCs studied may vary slightly in the time course of events following caveolin-1 knockdown and incubation in osteogenic medium, therefore time course studies in individual donor populations may help to decipher if there are significant differences in cell signaling occurring in caveolin-1 knockdown samples. There may also be sex dependent responses to caveolin-1 knockdown that have affected our results. Meanwhile, caveolin-1 knockdown in this study may have induced changes that less directly affect cell signaling pathways. For example, the enhanced ALP activity we observed in osteogenically induced caveolin-1 knockdown cells could have resulted from enhanced cell surface exposure of ALP, perhaps due to decreased caveolae/changes to the membrane topology accompanying caveolin-1 knockdown.

In other gene expression analysis not presented here, we found that there was a trend toward decreased expression of POU class 5 homeobox 1 (*POU5F/OCT4*) in MSCs transfected with caveolin-1 siRNA. This trend was observed in 4/6 donor populations tested, and in one donor population this trend reached statistical significance (data not shown). Although the expression level of *POU5F/OCT4* in MSCs is relatively very low compared to that in pluripotent cells (data not shown), the downregulation of *POU5F1/OCT4* in caveolin-1 siRNA transfected cells may reflect MSC progression towards a ''pre-differentiation state'' upon caveolin-1 knockdown that confers cells with an increased tendency to respond to osteogenic stimuli. Interestingly, others have found that treatment of mouse ES cells with caveolin-1 siRNA decreased expression of Oct4 mRNA and protein, as well as mRNA for other markers of pluripotency, namely Sox2, FoxD3, and Rex1 [Lee et al., 2010].

Further studies are clearly needed to validate and extend our findings. We have observed variability in the different donor MSC populations studied, both in Alizarin red staining and gene expression changes in our experiments. This could be related to basal caveolin-1 expression, variability in osteogenic potential, and variability in time course and dose responses.

In conclusion, our results strongly suggest that caveolin-1 may act as a functional antagonist to both human MSC self-renewal and osteogenic differentiation, and caveolin-1 expression increases in differentiated cells to stabilize the cell phenotype and reduce responsiveness to differentiation stimuli. Further investigation into how caveolae structures regulate cell signaling in these cells should provide insights into the cellular and molecular control of cell fate in adult stem cells.

ACKNOWLEDGMENTS

This study was supported in part by the Intramural Research Program of the National Institutes of Health (Z01 AR 41131) and the Commonwealth of Pennsylvania Department of Health. The authors would like to thank Dr. Bing Wang for technical assistance, Jian Tan for assistance isolating MSCs, Dr Naiqian Cheng for help with electron microscopy, and Dr Paul Manner (University of Washington) for providing human tissues.

REFERENCES

Case N, Xie Z, Sen B, Styner M, Zou M, O'Conor C, Horowitz M, Rubin J. 2010. Mechanical activation of beta-catenin regulates phenotype in adult murine marrow-derived mesenchymal stem cells. J Orthop Res 28:1531–1538.

Conrad PA, Smart EJ, Ying YS, Anderson RG, Bloom GS. 1995. Caveolin cycles between plasma membrane caveolae and the Golgi complex by microtubule-dependent and microtubule-independent steps. J Cell Biol 131:1421–1433.

Du J, Chen X, Liang X, Zhang G, Xu J, He L, Zhan Q, Feng XQ, Chien S, Yang C. 2011. Integrin activation and internalization on soft ECM as a mechanism of induction of stem cell differentiation by ECM elasticity. Proc Natl Acad Sci USA 108:9466–9471.

Dupree P, Parton RG, Raposo G, Kurzchalia TV, Simons K. 1993. Caveolae and sorting in the trans-Golgi network of epithelial cells. EMBO J 12:1597–1605.

Engelman JA, Wykoff CC, Yasuhara S, Song KS, Okamoto T, Lisanti MP. 1997. Recombinant expression of caveolin-1 in oncogenically transformed cells abrogates anchorage-independent growth. J Biol Chem 272:16374–16381.

Fra AM, Williamson E, Simons K, Parton RG. 1995. De novo formation of caveolae in lymphocytes by expression of VIP21-caveolin. Proc Natl Acad Sci USA 92:8655–8659.

Galbiati F, Volonte D, Engelman JA, Watanabe G, Burk R, Pestell RG, Lisanti MP. 1998. Targeted downregulation of caveolin-1 is sufficient to drive cell transformation and hyperactivate the p42/44 MAP kinase cascade. EMBO J 17:6633–6648.

Galbiati F, Volonte D, Brown AM, Weinstein DE, Ben-Ze'ev A, Pestell RG, Lisanti MP. 2000. Caveolin-1 expression inhibits Wnt/beta-catenin/Lef-1 signaling by recruiting beta-catenin to caveolae membrane domains. J Biol Chem 275:23368–23377.

Galbiati F, Volonte D, Liu J, Capozza F, Frank PG, Zhu L, Pestell RG, Lisanti MP. 2001. Caveolin-1 expression negatively regulates cell cycle progression

by inducing G(0)/G(1) arrest via a p53/p21(WAF1/Cip1)-dependent mechanism. Mol Biol Cell 12:2229–2244.

Griffoni C, Spisni E, Santi S, Riccio M, Guarnieri T, Tomasi V. 2000. Knockdown of caveolin-1 by antisense oligonucleotides impairs angiogenesis in vitro and in vivo. Biochem Biophys Res Commun 276:756–761.

Jasmin JF, Yang M, Iacovitti L, Lisanti MP. 2009. Genetic ablation of caveolin-1 increases neural stem cell proliferation in the subventricular zone (SVZ) of the adult mouse brain. Cell Cycle 8:3978–3983.

Kandror KV, Stephens JM, Pilch PF. 1995. Expression and compartmentalization of caveolin in adipose cells: Coordinate regulation with and structural segregation from GLUT4. J Cell Biol 129:999–1006.

Kolf CM, Cho E, Tuan RS. 2007. Mesenchymal stromal cells. Biology of adult mesenchymal stem cells: Regulation of niche, self-renewal and differentiation. Arthritis Res Ther 9:204.

Krajewska WM, Maslowska I. 2004. Caveolins: Structure and function in signal transduction. Cell Mol Biol Lett 9:195–220.

Lee MY, Ryu JM, Lee SH, Park JH, Han HJ. 2010. Lipid rafts play an important role for maintenance of embryonic stem cell self-renewal. J Lipid Res 51:2082–2089.

Li J, Hassan GS, Williams TM, Minetti C, Pestell RG, Tanowitz HB, Frank PG, Sotgia F, Lisanti MP. 2005. Loss of caveolin-1 causes the hyper-proliferation of intestinal crypt stem cells, with increased sensitivity to whole body gamma-radiation. Cell Cycle 4:1817–1825.

Lisanti MP, Scherer PE, Tang Z, Sargiacomo M. 1994. Caveolae, caveolin and caveolin-rich membrane domains: A signalling hypothesis. Trends Cell Biol 4:231–235.

Lofthouse RA, Davis JR, Frondoza CG, Jinnah RH, Hungerford DS, Hare JM. 2001. Identification of caveolae and detection of caveolin in normal human osteoblasts. J Bone Joint Surg Br 83:124–129.

Lu Z, Ghosh S, Wang Z, Hunter T. 2003. Downregulation of caveolin-1 function by EGF leads to the loss of E-cadherin, increased transcriptional activity of beta-catenin, and enhanced tumor cell invasion. Cancer Cell 4:499–515.

Mo S, Wang L, Li Q, Li J, Li Y, Thannickal VJ, Cui Z. 2010. Caveolin-1 regulates dorsoventral patterning through direct interaction with beta-catenin in zebrafish. Dev Biol 344:210–223.

Monier S, Parton RG, Vogel F, Behlke J, Henske A, Kurzchalia TV. 1995. VIP21-caveolin, a membrane protein constituent of the caveolar coat, oligomerizes in vivo and in vitro. Mol Biol Cell 6:911–927.

Murata M, Peranen J, Schreiner R, Wieland F, Kurzchalia TV, Simons K. 1995. VIP21/caveolin is a cholesterol-binding protein. Proc Natl Acad Sci USA 92:10339–10343.

Nesti LJ, Jackson WM, Shanti RM, Koehler SM, Aragon AB, Bailey JR, Sracic MK, Freedman BA, Giuliani JR, Tuan RS. 2008. Differentiation potential of multipotent progenitor cells derived from war-traumatized muscle tissue. J Bone Joint Surg Am 90:2390–2398.

Nohe A, Keating E, Underhill TM, Knaus P, Petersen NO. 2005. Dynamics and interaction of caveolin-1 isoforms with BMP-receptors. J Cell Sci 118:643–650.

Palade GE. 1953. Fine structure of blood capillaries. J Appl Phys 24:1424–1424.

Park JS, Kim HY, Kim HW, Chae GN, Oh HT, Park JY, Shim H, Seo M, Shin EY, Kim EG, Park SC, Kwak SJ. 2005. Increased caveolin-1, a cause for the declined adipogenic potential of senescent human mesenchymal stem cells. Mech Ageing Dev 126:551–559.

Park JH, Lee MY, Han HJ. 2009. A potential role for caveolin-1 in estradiol-17beta-induced proliferation of mouse embryonic stem cells: Involvement of Src, PI3K/Akt, and MAPKs pathways. Int J Biochem Cell Biol 41:659–665.

Patel HH, Murray F, Insel PA. 2008. Caveolae as organizers of pharmacologically relevant signal transduction molecules. Annu Rev Pharmacol Toxicol 48:359–391.

Petrie Aronin CE, Tuan RS. 2010. Therapeutic potential of the immunomodulatory activities of adult mesenchymal stem cells. Birth Defects Res C Embryo Today 90:67–74.

Pricola KL, Kuhn NZ, Haleem-Smith H, Song Y, Tuan RS. 2009. Interleukin-6 maintains bone marrow-derived mesenchymal stem cell stemness by an ERK1/2-dependent mechanism. J Cell Biochem 108:577–588.

Razani B, Engelman JA, Wang XB, Schubert W, Zhang XL, Marks CB, Macaluso F, Russell RG, Li M, Pestell RG, Di Vizio D, Hou H, Jr, Kneitz B, Lagaud G, Christ GJ, Edelmann W, Lisanti MP. 2001. Caveolin-1 null mice are viable but show evidence of hyperproliferative and vascular abnormalities. J Biol Chem 276:38121–38138.

Ren J, Jin P, Sabatino M, Balakumaran A, Feng J, Kuznetsov SA, Klein HG, Robey PG, Stroncek DF. 2011. Global transcriptome analysis of human bone marrow stromal cells (BMSC) reveals proliferative, mobile and interactive cells that produce abundant extracellular matrix proteins, some of which may affect BMSC potency. Cytotherapy 13:661–674.

Rodriguez DA, Tapia JC, Fernandez JG, Torres VA, Munoz N, Galleguillos D, Leyton L, Quest AF. 2009. Caveolin-1-mediated suppression of cyclooxygenase-2 via a beta-catenin-Tcf/Lef-dependent transcriptional mechanism reduced prostaglandin E2 production and survivin expression. Mol Biol Cell 20:2297–2310.

Rothberg KG, Heuser JE, Donzell WC, Ying YS, Glenney JR, Anderson RG. 1992. Caveolin, a protein component of caveolae membrane coats. Cell 68:673–682.

Rubin J, Schwartz Z, Boyan BD, Fan X, Case N, Sen B, Drab M, Smith D, Aleman M, Wong KL, Yao H, Jo H, Gross TS. 2007. Caveolin-1 knockout mice have increased bone size and stiffness. J Bone Miner Res 22:1408–1418.

Scherer PE, Lisanti MP, Baldini G, Sargiacomo M, Mastick CC, Lodish HF. 1994. Induction of caveolin during adipogenesis and association of GLUT4 with caveolin-rich vesicles. J Cell Biol 127:1233–1243.

Scherer PE, Okamoto T, Chun M, Nishimoto I, Lodish HF, Lisanti MP. 1996. Identification, sequence, and expression of caveolin-2 defines a caveolin gene family. Proc Natl Acad Sci USA 93:131–135.

Schwab W, Galbiati F, Volonte D, Hempel U, Wenzel KW, Funk RH, Lisanti MP, Kasper M. 1999. Characterisation of caveolins from cartilage: Expression of caveolin-1, -2 and -3 in chondrocytes and in alginate cell culture of the rat tibia. Histochem Cell Biol 112:41–49.

Schwab W, Kasper M, Gavlik JM, Schulze E, Funk RH, Shakibaei M. 2000. Characterization of caveolins from human knee joint catilage: Expression of caveolin-1, -2, and -3 in chondrocytes and association with integrin beta1. Histochem Cell Biol 113:221–225.

Solomon KR, Adolphson LD, Wank DA, McHugh KP, Hauschka PV. 2000. Caveolae in human and murine osteoblasts. J Bone Miner Res 15:2391–2401.

Song KS, Li S, Okamoto T, Quilliam LA, Sargiacomo M, Lisanti MP. 1996a. Co-purification and direct interaction of Ras with caveolin, an integral membrane protein of caveolae microdomains. Detergent-free purification of caveolae microdomains. J Biol Chem 271:9690–9697.

Song KS, Scherer PE, Tang Z, Okamoto T, Li S, Chafel M, Chu C, Kohtz DS, Lisanti MP. 1996b. Expression of caveolin-3 in skeletal, cardiac, and smooth muscle cells. Caveolin-3 is a component of the sarcolemma and co-fractionates with dystrophin and dystrophin-associated glycoproteins. J Biol Chem 271:15160–15165.

Sotgia F, Williams TM, Cohen AW, Minetti C, Pestell RG, Lisanti MP. 2005. Caveolin-1-deficient mice have an increased mammary stem cell population with upregulation of Wnt/beta-catenin signaling. Cell Cycle 4:1808–1816.

Tang Z, Scherer PE, Okamoto T, Song K, Chu C, Kohtz DS, Nishimoto I, Lodish HF, Lisanti MP. 1996. Molecular cloning of caveolin-3, a novel member of the caveolin gene family expressed predominantly in muscle. J Biol Chem 271:2255–2261.

Torres VA, Tapia JC, Rodriguez DA, Lladser A, Arredondo C, Leyton L, Quest AF. 2007. E-cadherin is required for caveolin-1-mediated down-regulation of the inhibitor of apoptosis protein survivin via reduced beta-catenin-Tcf/Lef-dependent transcription. Mol Cell Biol 27:7703–7717.

Volonte D, Zhang K, Lisanti MP, Galbiati F. 2002. Expression of caveolin-1 induces premature cellular senescence in primary cultures of murine fibroblasts. Mol Biol Cell 13:2502–2517.

Wertz JW, Bauer PM. 2008. Caveolin-1 regulates BMPRII localization and signaling in vascular smooth muscle cells. Biochem Biophys Res Commun 375:557–561.

Yamada E. 1955. The fine structure of the gall bladder epithelium of the mouse. J Biophys Biochem Cytol 1:445–458.